

# Estimation of a Plasma Mirror Reflectivity of LFEX Laser and Relevant Results Using Electron Energy Spectrometers<sup>\*)</sup>

Tetsuo OZAKI, Eisuke MIURA<sup>1)</sup>, Sadaoki KOJIMA<sup>2)</sup>, Yasunobu ARIKAWA<sup>3)</sup>, Yuuki ABE<sup>3)</sup>, Kohei YAMANOI<sup>3)</sup>, Tomokazu IKEDA<sup>3)</sup>, Katsuhiro ISHII<sup>4)</sup>, Atsushi SUNAHARA<sup>5)</sup>, Tomoyuki JOHZAKI<sup>6)</sup>, Hiroshi SAWADA<sup>7)</sup>, Shinsuke FUJIOKA<sup>3)</sup>, Hitoshi SAKAGAMI, Yoneyoshi KITAGAWA<sup>4)</sup> and Yoshitaka MORI<sup>4)</sup>

*National Institute for Fusion Science, 322-6 Oroshi, Toki, Gifu 509-5292, Japan*

<sup>1)</sup>*National Institute of Advanced Industrial Science and Technology,*

*1-1-1 Umezono, Tsukuba, Ibaraki 305-8560, Japan*

<sup>2)</sup>*National Institutes for Quantum and Radiological Science and Technology,*

*8-1-7 Umemidai, Kizugawa-shi, Kyoto 619-0215, Japan*

<sup>3)</sup>*Institute of Laser Engineering, Osaka University, 2-6 Yamada-oka, Suita, Osaka 565-0871, Japan*

<sup>4)</sup>*The Graduate School for the Creation of New Photonics Industries,*

*1955-1 Kurematsu-cho, Nishi-ku, Hamamatsu, Shizuoka 431-1202, Japan*

<sup>5)</sup>*Purdue University, 610 Purdue Mall, West Lafayette, IN, 47907, United States*

<sup>6)</sup>*Hiroshima University, 1-3-2 Kagamiyama, Higashihiroshima, Hiroshima 739-8511, Japan*

<sup>7)</sup>*University of Nevada, Reno, 1664 N. Virginia Street, Reno, NV 89557, United States*

(Received 10 January 2022 / Accepted 17 May 2022)

In the counter-irradiation, which is one of the fast ignition schemes, higher core energy coupling can be expected when there are two hot electron flows in counter directions. Two plasma mirrors were installed for the counter irradiation at about 180 degrees. The hot electron effective temperatures ( $T_{eff}$ ) were measured by using electron energy spectrometers.  $T_{eff}$  vs the laser intensity on a foil target followed Wilkes' scaling law. The energy incident on the target could be calculated by estimating the laser intensity on the target from  $T_{eff}$  and estimating the focusing radius from the X-ray pinhole camera image. As a result, the reflectivity could be estimated to be  $17 \pm 3\%$ .

© 2022 The Japan Society of Plasma Science and Nuclear Fusion Research

Keywords: plasma mirror, ESM, Wilks' scaling, LFEX, effective temperature, counter irradiation, fast ignition

DOI: 10.1585/pfr.17.2404084

## 1. Introduction

Fast ignition [1–3] is one of the inertial fusions, performed by additional heating of an imploded core. The realization of conventional inertial fusion requires compression of 1000 times the solid density and ignition at the final stage of implosion. This requires a huge amount of laser energy. Since fast ignition performs implosion and ignition in an independent process, it can be expected that the required energy can be reduced with relatively weak compression.

Fast ignition may be performed on one side or the other sides when additional heating is applied to the implosion core. In the former case it is relatively easy to design lasers and targets. However, the latter has a complicated structure, which is proposed by The Graduate School for the Creation of New Photonics Industries (GPI) [4]. In a case of counter-irradiation, Weibel instability creates a complex magnetic field [5] which is expected to be an effi-

cient confinement while the physical process is underway.

By counter irradiating, hot electrons also run in counter directions. This causes the Weibel instability and creates a complex magnetic field around the core. Hot electrons are trapped around this magnetic field and heat the core efficiently. Such a phenomenon can be expected when the laser intensity is  $10^{18}$  W/cm<sup>2</sup> or more. On the other hand, if it is  $10^{17}$  W/cm<sup>2</sup> or less, shock wave heating can be expected.

The laser at GPI is low intensity. Therefore, we carried out the experiment with one of the world's largest heating lasers, the LFEX. LFEX has 4-beam bundles with rectangular shapes. However, it is designed as only a one side injection device. Two of the four beams are reflected by mirrors and irradiate to the target. On the other hand, the pre-pulse removal is a challenge when using high intensity lasers for additional heating. If the pre-formed plasma produced by the pre-pulse is large, the energy of the hot electrons becomes too large, and the heating efficiency decreases. Therefore, instead of using normal mirrors, a

author's e-mail: ozaki@nifs.ac.jp

<sup>\*)</sup> This article is based on the presentation at the 30th International Toki Conference on Plasma and Fusion Research (ITC30).

plasma mirror is used to remove the pre-pulse [6].

The LFEX lasers are designed to be unilaterally incident, so each beam cannot swing significantly. It is an easy way to install plasma mirrors close to the target. The problem is that the intensity of the laser on the plasma mirrors is extremely strong, more than two orders of magnitude higher than the intensity conventionally used. Here we will consider whether the plasma mirror works well with such strength. For this purpose, it is important to measure the reflectivity of the plasma mirror.

## 2. Experimental Setup

The experiment was conducted using an LFEX laser [7] (port-through energy about 1 kJ) at The Institute of Laser Engineering, Osaka University. The LFEX is a 4-beam bundle that comes from port 52 (p52). Each of the four beams can be operated independently. However, it cannot be irradiated at a large swing, since it is also used as a one pulse compressor.

As shown in Fig. 1, the beams are divided into two and irradiate the two plasma mirrors. The plasma mirrors are 2 mm × 2 mm glass plates and are installed at 190 degrees, 3 mm away from the target. This is because the counter light does not damage the other optical component, so each irradiation of 5 degrees is tilted.

The target used was a deuterium thin polyethylene film (10 μm and 100 μm thick) containing copper. The 10 μm target was for observing heating and 100 μm target was for observing the effect of counter irradiation in detail. The generated number of hot electrons could be estimated by observing the  $K_{\alpha}$  at which electrons hit copper. Contained deuterium was for DD neutron measurement.

The measurement arrangement is shown in Fig. 2. The LFEX laser is injected toward the center of through the plasma mirrors near the target. Hot electrons are measured by three electron energy spectrometers (ESM) [8]. The three ESMs are installed, behind the two plasma mirrors on the opposite side of the LFEX, 20.9 degrees (from the LFEX traveling direction, p43) and the sides perpendicular to the LFEX, 90 degrees (p34 and p35) (Fig. 3). ESM avoids the influence of strong X-rays from the target by arranging permanent magnets in parallel along the X-

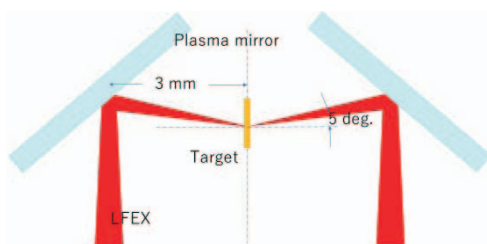


Fig. 1 Plasma mirrors. Two plasma mirrors installed at 3 mm distance from target. Injection angle of each beam 5 degrees from target normally due to protection of component from back scattering of LFEX.

ray direction. By minimizing the magnetic field leakage, it is possible to measure electron spectra from 0.5 MeV to 120 MeV and protons or deuteron ions up to 7 MeV. An imaging plate (IP) is used as the detector.

Three XPHCs [9] are installed at 138.2 (p24), 109.5 (p26) and 138.2 degrees (p56). These are for observing the focused diameter of the target. Two HOPGs [10] ( $K_{\alpha}$  measurements) are installed at 109.5 (p41) and 159.1 degrees (p44). The electron beam intensity is observed from the absolute amount of  $K_{\alpha}$  and the temperature rise from the line near  $K_{\alpha}$ . A Mandala [11] neutron measuring instrument is installed 15 m outside 125.3 degrees (p37). This mainly measures DD neutrons of the thermal and laser accelerated beam-target.

Figure 3 shows the plasma mirror and target from the ESM. The installation positions of the ESMs are carefully selected so that the generated electron and ion beams are not hidden by mirrors and other components. Alignment is performed in advance in a similar optical system outside the chamber.

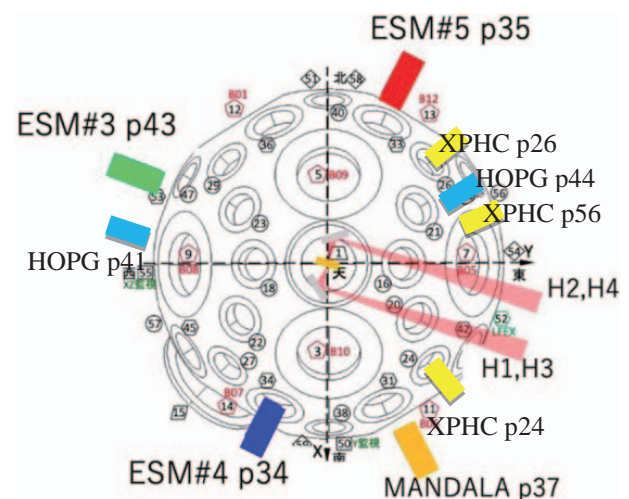


Fig. 2 Diagnostic arrangements. Three ESMs installed in forward direction (ESM#3), and two vertical directions (ESM#4 and #5). XPHCs for spot size monitors. HOPGs are X-ray spectrometers. MANDALA is neutron time-of-flight detector.

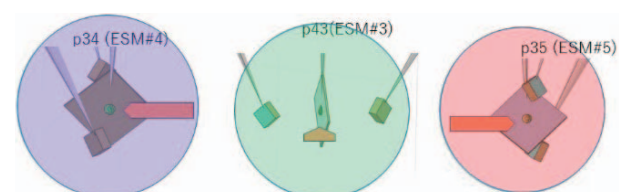


Fig. 3 Viewing sights from ESMs. Viewing sights from ESM#4, #3 and #5 left, center, right, Two plasma mirrors and target shown. Red arrows indicate LFEX direction.

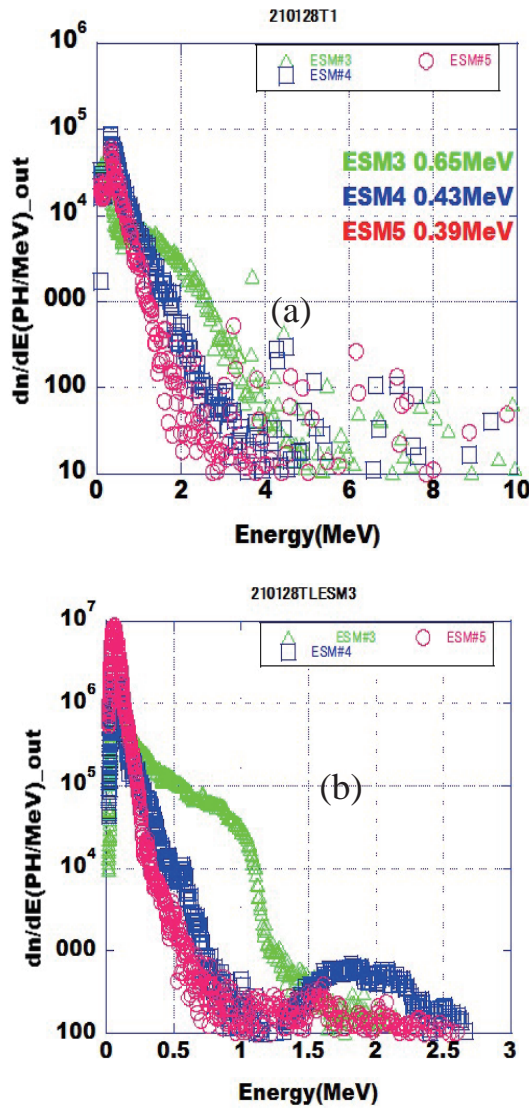


Fig. 4 Electron and Ion spectra. (a) Electron spectra, Vertical  $T_{\text{eff}}$  (ESM#3) becomes slightly high. (b) Ion spectra, Ion component estimated about 80% deuterium. Vertical Ion flux also becomes high.

### 3. Experimental Results

Figure 4 (a) shows a typical ion energy spectrum in the counter-irradiation. ESM#4 and ESM#5 are observed from the axial direction of the laser reflected by the plasma mirror. ESM#3 is observed from a direction perpendicular to the laser irradiation axis.

When the  $10\mu\text{m}$  target is irradiated with the same laser intensity on the left and right, the electron spectra of ESM#4 and ESM#5 are almost the same. However, the electron spectrum of ESM#3 is different.  $T_{\text{eff}}$  in ESM#3 becomes high. This may suggest that hot electrons are captured by the magnetic field due to Weibel instability and accelerated in the plasma [12].

Figure 4 (b) shows the spectrum of ions. Hydrogen adsorbed on the surface is generated as protons, although the target contains deuterium polyethylene. Ions cannot distin-

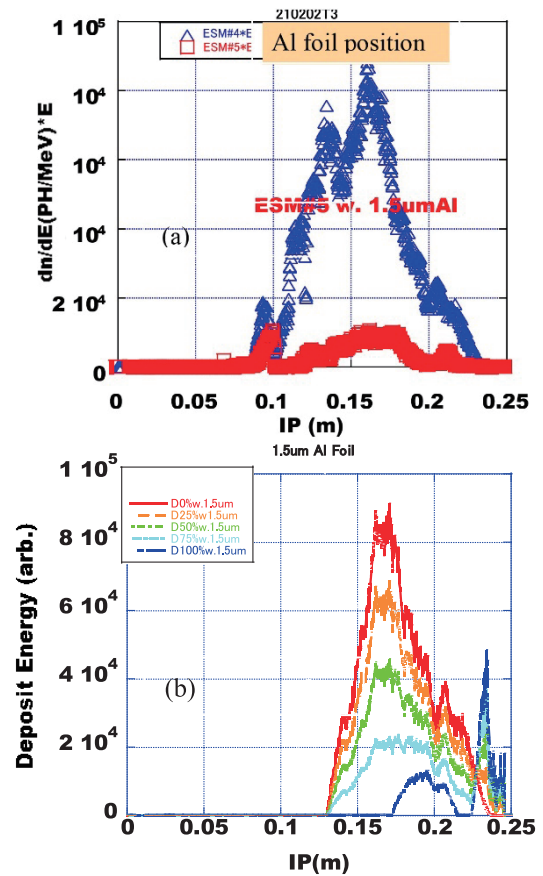


Fig. 5 on spectra with/without  $1.5\mu\text{m}$  Al foil. (a) Experimental results.  $1.5\mu\text{m}$  Al foil covered from 0.1 m to 0.2 m on IP. (b) Calculation results based on results without Al foil. Ions enter foil at oblique angle. Therefore, start position of track on IP clearly different by HD ratio.

guish between protons and deuterons in the ESM. This is because particles with the same momentum draw the same orbit because the energy analysis is performed only with the magnetic field. We attached  $1.5\mu\text{m}$  of aluminium foil on ESM#5 and compared the difference in the track on the IP of ESM#4 without aluminium foil (Fig. 5 (a)). Al foil was attached on IP by the self-static electricity. Here, ions with the same energy distribution are assumed to be observed in ESM#4 and ESM#5. We assume that there is no energy dependence of the hydrogen-deuterium (HD, =  $D/(D+H)$ ) ratio. The spectrum of ESM#4 is varied by a HD ratio scan with  $1.5\mu\text{m}$  of aluminium foil in the calculation (Fig. 5 (b)). The calculated spectrum matches the spectrum obtained by ESM # 5 when the deuterium concentration can be estimated to be about 80%.

Ions in ESM#3 were also increased as electrons. This is because the ions compensate for the potential of hot electrons escaping.

Neutrons are generated mainly from the DD reaction between beam deuterons, which are by laser acceleration and deuterons in the target. The average energy of ions can be obtained from their spectrum. The neutron energy

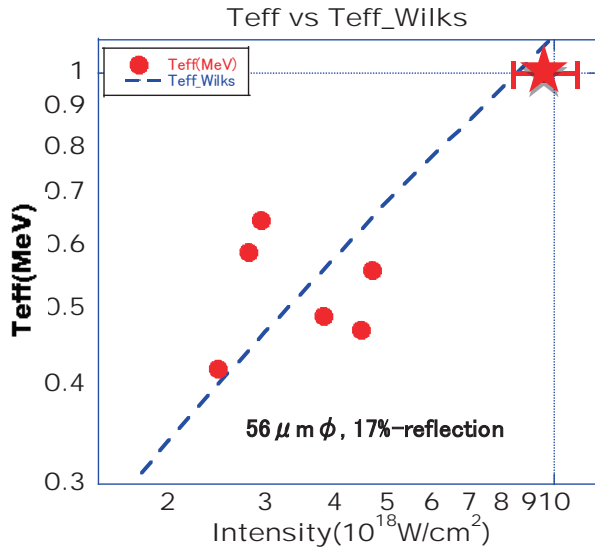


Fig. 6  $T_{eff}$  vs Laser intensity.  $T_{eff}$  in direct irradiation assumed on Wilks' scaling (broken line). Error bar on star (direct irradiation without plasma mirrors) comes from XPHC data ambiguity. Other data have small errors when reflectivity determined.

spectrum, which is calculated from the energy of ions is in good agreement with the experiment results [13].

When the laser intensity asymmetrically irradiates the  $10\ \mu\text{m}$  target on the left and right sides,  $T_{eff}$  on the stronger side increases and the ions increase. In a case of such asymmetry, there is no increase compared to  $T_{eff}$  and ion flux on the perpendicular direction (ESM#3) in symmetrical irradiation.  $T_{eff}$  becomes low at the  $100\ \mu\text{m}$  target when observed in the perpendicular direction. This is because the thick target reduces the electron current density that forms the magnetic field, due to Weibel instability. If one side is delayed by 50 ps at the  $100\ \mu\text{m}$  target, plasma acceleration will occur and  $T_{eff}$  will increase because the delayed laser is incident in pre-formed plasma.

Figure 6 plots the laser intensity on the target on the horizontal axis and  $T_{eff}$  on the vertical axis. Several scalings [14, 15] have been proposed for the relationship between laser intensity and  $T_{eff}$  at high intensity short pulses. Wilks' scaling [16] is closest to the condition in this case.

(broken line in Fig. 6). We adopted  $T_{eff}$  on the opposite side of the laser irradiation.

The star in Fig. 6 indicates  $T_{eff}$  when the target was directly irradiated without using the plasma mirror. At this time, the XPHC data was  $56 \pm 4\ \mu\text{m}\phi$ . Next, the reflectivity was changed to fit  $T_{eff}$  obtained in the experiment to Wilks' scaling. The results correspond to a reflectivity of  $17 \pm 3\%$ .

## 4. Summary

Counter-irradiation is one of the fast ignition schemes. It can be expected to increase heating efficiency by trapping hot electrons in the magnetic field caused by Weibel instability. Here, the high-intensity laser, LFEX is used to realize counter-irradiation, using plasma mirrors near the target. The irradiation intensity of the plasma mirrors is around  $10^{18}\ \text{W}/\text{cm}^2$ . The reflectivity can be observed to be  $17 \pm 3\%$  assuming Wilks' scaling by using ESMs.

## Acknowledgements

This work is supported by NIFS14KUGK120, KUGK129, NIFS-URXS302, URXS305, IHH001 and The Graduate School for the Creation of New Photonics Industries.

- [1] M. Tabak *et al.*, Phys. Plasmas **1**, 1626 (1994).
- [2] Y. Kitagawa *et al.*, Phys. Rev. Lett. **114**, 195002 (2015).
- [3] R. Kodama *et al.*, Nature **418**, 933 (2002).
- [4] Y. Mori *et al.*, Nucl. Fusion **57**, 116031 (2017).
- [5] Y. Mori *et al.*, Phys. Rev. Lett. **117**, 055001 (2016).
- [6] Y. Arikawa, *et al.*, Appl. Opt. **55**, 6850 (2016).
- [7] H. Shiraga *et al.*, Plasma Phys. Control. Fusion **53**, 124029 (2011).
- [8] T. Ozaki *et al.*, Rev. Sci. Instrum. **83**, 10D920 (2012).
- [9] E. Miura *et al.*, HED Phys. **36**, 100890 (2020).
- [10] S. Sakata *et al.*, Nature Comm. **8**, 3937 (2018).
- [11] Y. Abe *et al.*, Rev. Sci. Instrum. **89**, 110I114 (2018).
- [12] S. Kojima *et al.*, Comm. Phys. **2**, 99 (2019).
- [13] Y. Abe *et al.*, HED Phys. **36**, 100803 (2020).
- [14] M.G. Haines *et al.*, Phys. Rev. Lett. **102**, 045008 (2009).
- [15] S. Gordienko, A. Pukov *et al.*, Phys. Plasmas **12**, 043109 (2005).
- [16] S.C. Wilks *et al.*, Phys. Rev. Lett. **69**, 1383 (1992).